Photoemission studies of the initial adsorption and growth of Ag and Au on Ge and Si

A. L. Wachs, T. Miller, A. P. Shapiro, and T. -C. Chiang
Department of Physics and Materials Research Laboratory, University of Illinois at Urbana-Champaign, 1110 West Green Street, Urbana, Illinois 61801
(Received 9 October 1986)

High-resolution core-level and valence-band photoemission studies have been performed to investigate the initial phases of growth of Ag on Si(111)-(7×7) and Ge(111)-$c(2\times8)$, and Au on Ge(111)-$c(2\times8)$. These systems were also studied with electron diffraction. Upon the deposition of various amounts of Ag or Au on the Si and Ge substrates, the photoemission spectra exhibited selective modifications of surface states and individual core-level components corresponding to different atomic sites. The results establish correlations between the electronic and structural properties of the substrate surfaces and have implications for possible growth models of Au and Ag upon them.

I. INTRODUCTION

In recent years the study of the structural and electronic properties of semiconductor surfaces and of thin metallic films deposited upon them has become a topic of great interest.[1–8] These systems have been studied extensively by many methods, such as photoemission, electron diffraction, Auger-electron spectroscopy, scanning electron microscopy, Rutherford backscattering, and scanning tunneling microscopy (STM). These methods, all somewhat complementary but limited in scope, have provided information on the chemical composition and structural and electronic properties in the near-surface region. Despite the many advances made in this field, a detailed picture is still lacking of the adsorption and growth behavior for most, if not all, metal-semiconductor systems.

In this paper, we report experimental investigations of the initial phases of the growth of three related metal-semiconductor systems: Ag on Si(111)-(7×7), Ag on Ge(111)-$c(2\times8)$, and Au on Ge(111)-$c(2\times8)$ by means of electron diffraction, and high-resolution core-level and valence-band photoemission. The results for a related system, Ag on Ge(100), have been reported before.[8] Core-level binding energies depend on the local atomic environments; thus high-resolution spectra may contain information about the presence or absence of atoms in inequivalent sites.[9–11] This effect has been observed in many cases. For example, surface atoms of single crystals generally show binding-energy shifts relative to the bulk atoms. With the deposition of metals on the surface, the core-level components may be selectively modified depending on the detailed mechanism and configuration of adsorption and growth. Valence-band photoemission is a measure of the density of states (DOS), bulk and surface. By investigating possible selective modifications of the various states by metal deposition at various coverages, the substrate surface-specific features can be identified. Our results establish correlations between structural and electronic properties. They provide useful information in relation to Si(111)-(7×7) and Ge(111)-$c(2\times8)$ surface structural models, and have implications for possible Au and Ag adsorption and growth models upon these surfaces.

This paper is organized as follows. We discuss the experimental details in Sec. II. Results and discussion for each of the three systems studied are presented in Sec. III; reflection high-energy electron diffraction (HEED) results, core-level, and valence-band photoemission data are presented separately. Section IV contains the summary and conclusions.

II. EXPERIMENTAL DETAILS

The photoemission measurements were performed at the Synchrotron Radiation Center of the University of Wisconsin—Madison. Synchrotron radiation was dispersed by either a Mark V "Grasshopper" monochromator or a 3-m toroidal grating monochromator. A double-pass cylindrical mirror analyzer detected electrons emitted from the sample. High-resolution measurements of valence-band DOS and Ge and Si core levels were made with an overall resolution of about 0.2—0.4 eV depending on the photon energy. Peak counts for the core-level spectra were typically on the order of 1500 counts/sec. The energy position of the substrate Fermi level was obtained by measuring the Fermi-level position of a gold foil in electrical contact with the substrate.

Si(111)-(7×7) substrates were formed from n- and p-type wafers cut into rectangles of about 13×5 mm. Heating of the sample was accomplished by passing current directly through it. Samples were cleaned in the usual manner, namely, by flashing to about 1250 °C, after which HEED gave a very sharp (7×7) pattern. The sample temperature was measured with an infrared pyrometer. Sample surface quality was judged by the HEED background and by the sharpness of the well-known surface states near the Fermi edge in the photoemission spectra.[12–16]

The p-type Ge(111) sample was aligned by Laue diffraction to within 1° and mechanically polished to a mirror finish. Prior to insertion in the vacuum chamber, the sample was etched in dilute NaOCl. The clean, nominally $c(2\times8)$ reconstructed surface was obtained by repeated cycles of sputtering and annealing to 800 °C. The sample temperature was monitored by means of a thermocouple

junction attached on its back side. HEED from the sample surface displayed sharp one-eighth order spots and a low background. Surface cleanliness was confirmed by Auger spectroscopy and examination of surface-state and valence-band photoemission spectra. The spectra were in excellent agreement with previously reported data.[15,16]

The Au and Ag deposited upon these samples came from a small tungsten crucible and a small tantalum crucible, respectively, heated by electron beam bombardment. The deposit thickness was determined using a quartz-crystal thickness monitor. For the small coverages this monitor determined rates of evaporation through repeated timings. Once calibrated, the thickness was established by controlling the length of time the shutter was open. HEED was used to examine all Au and Ag films prepared for photoemission. The film cleanliness was verified by Auger electron spectroscopy. Specific results for each system will be reported below.

III. RESULTS AND DISCUSSION

A. Ag on Si(111)-(7×7)

1. HEED

Diffraction patterns of the clean Si(111)-(7×7) surface were of high contrast and low background, an indication of good surface quality. The deposition of Ag was done at substrate temperatures of about 70 °C. The background increased after deposition of 0.25 Ag(111) monolayer (ML), but no Ag(111) lines could be seen. A ML of Ag is defined as an atomic layer in Ag(111), or 1.38×10^{15} atoms/cm^2. Surfaces covered with 0.5 Ag(111) ML had the (7×7) substrate diffraction pattern, somewhat higher background, and extremely faint, extra spots derived from Ag(111) in parallel epitaxy with the substrate. Here, parallel epitaxy means that the overlayer crystallographic axes are parallel to the corresponding axes of the substrate. At 0.75 ML Ag coverage, the background was high, the (7×7) substrate diffraction pattern became very weak, and fuzzy Ag(111) streaks became readily visible. Sharper Ag(111) streaks and weak Si(111)-(1×1) spots appeared at one ML of Ag coverage. At higher coverages substrate diffraction features were no longer visible. The Ag(111) streaks continued to appear in parallel epitaxy and became very sharp on a low background for coverages equal to just a few monolayers. Many prepared Ag films showed extremely weak (barely detectable) extra diffraction streaks corresponding to domains rotated 30° about the surface normal.[7] Overlayer growth appears to be fairly smooth at all of the coverages studied; no tilted Ag facets or three-dimensional structures were detected. Our detection limit of diffraction spots from tilted facets corresponds to a total facet area equivalent to about $\frac{1}{10}-\frac{1}{20}$ of the sample surface area. The high background appearing for coverages less than and about one monolayer is probably related to the small sizes of the islands and the effect of the strong, incommensurate substrate surface corrugation upon overlayer ordering. The substrate corrugation, a result of the very complicated surface reconstruction involving stacking faults and atomic displacements for several layers, is not necessarily substantially removed by the Ag adsorption, even for coverages that the (7×7) HEED pattern has disappeared. HEED is sensitive to essentially only the top atomic layer. The visual disappearance of the (7×7) HEED pattern for coverages more than about 1 ML does not necessarily imply that the reconstruction is substantially removed. Our findings are consistent with previous electron diffraction, photoemission, and Auger-electron spectroscopy studies showing the growth mode to be smooth but not exactly layer by layer near room temperature.[8,17]

2. Core levels

Figure 1 shows high-resolution scans of the Si 2*p* core level, taken at a photon energy of 130 eV, for both the clean Si(111)-(7×7) surface (bottom spectrum) and a Si(111) surface with 0.25 ML Ag deposited upon it (top spectrum). The dependence of electron mean-free path on energy causes these spectra to emphasize surface-related features.[9–11,18] Additional spectra emphasizing the bulk contribution were taken with 108-eV photons; these spectra are not shown here for simplicity.

In the clean spectrum, there are two features: the small

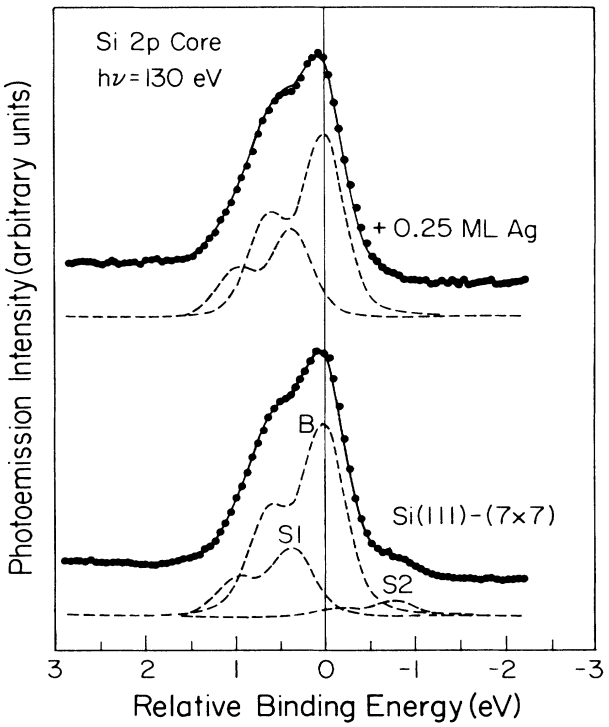

FIG. 1. Surface-sensitive photoemission spectra of the Si-2*p* core levels taken with $h\nu=130$ eV. The bottom spectrum is of clean Si(111)-(7×7); the top of Si(111) + 0.25 ML Ag. Circles are data points. The bottom solid curve is a fit to the data. The top solid curve is a model of the Ag-covered surface data (see text for details). The dashed curves indicate fit or model line shape components, offset vertically for clarity. Component *B* is bulk in origin; *S*1 and *S*2 are surface-derived. Binding energies are referred to component *B* of the clean-surface Si-$2p_{3/2}$ line.

shoulder on the low-binding-energy side of the doublet and the filling-in of the valley between the two spin-orbit-split peaks. These features have been observed and analyzed elsewhere.[18,19] They correspond to two surface components shifted relative to the bulk component.[19] The spectrum of the Ag-covered Si(111) surface, on the other hand, lacks the small low-binding-energy shoulder; otherwise, the two spectra appear quite similar.

The decomposition of the clean spectrum in Fig. 1 into the bulk (B) and the two surface ($S1$ and $S2$) components is indicated by the dashed curves. This was done by a nonlinear least-squares fitting procedure involving the simultaneous fit of the bulk- and surface-sensitive spectra as described in Ref. 19. The solid curve in Fig. 1 is the fit to the overall line shape. The relative binding-energy scale in Fig. 1 is referred to the bulk Si $2p_{3/2}$ line. The results of the fit are tabulated in Table I; they are in excellent agreement with the results of Ref. 19. The very small differences between the present results (Table I) and the results in Ref. 19 (Table I) indicate a high degree of reproducibility and provide an estimate of the uncertainty of our measurements (the two experiments were performed at different times on different samples; even the monochromators used for these two experiments were not necessarily the same).

TABLE I. Fitting parameters for the core-level spectra shown in Figs. 1 and 3. All energies are in eV. SS and BS refer to the surface- and bulk-sensitive spectra, respectively. The surface-sensitive spectra for the clean Ge(111)-$c(2\times8)$ surface were taken at incident photon energies of 70 and 90 eV; the SS fitting parameters for this system are listed for each photon energy respectively, the upper (lower) number referring to the 70-eV (90-eV) spectrum for each parameter. The branching ratio, in the case of Si, is the $2p_{1/2}$-to-$2p_{3/2}$ intensity ratio, and in the case of Ge, is the $3d_{3/2}$-to-$3d_{5/2}$ intensity ratio. The Lorentzian and Gaussian widths refer to the full width at half maximum. The binding energy shifts of the two surface components ($S1$ and $S2$) are referred to the bulk component in each case. The weights (relative intensities) of the bulk, $S1$, and $S2$ components add up to one.

	Ge $3d$ Ge(111)-$c(2\times8)$	Si $2p$ Si(111)-(7×7)
Spin-orbit splitting	0.586	0.612
Branching ratio (BS)	0.480	0.508
Branching ratio (SS)	0.618	0.527
	0.625	
Lorentzian width	0.150	0.156
Gaussian width (BS)	0.357	0.306
Gaussian width (SS)	0.378	0.454
	0.367	
Surface component $S1$		
Shift	0.260	−0.358
Weight (BS)	0.210	0.097
Weight (SS)	0.404	0.250
	0.477	
Surface component $S2$		
Shift	0.767	0.763
Weight (BS)	0.036	0.015
Weight (SS)	0.077	0.055
	0.092	

Recent STM and transmission electron microscopy studies indicated that the surface structure of Si(111)-(7×7) can be described fairly accurately by the dimer-adatom-stacking (DAS) fault model of Takayanagi *et al.*, which includes ($\frac{12}{49}$) Si(111) ML surfaces "adatoms."[20–23] Here, a Si(111) ML is defined to be 7.83×10^{14} atoms/cm^2, or one-half of a double Si(111) layer. The $S2$ and $S1$ components in the core-level spectra have been associated with emission from the adatoms and mainly the first full monolayer existing below the adatoms, respectively, because the relative intensities of $S2$ and $S1$ correspond closely to $\frac{12}{49}$ and 1 ML, respectively.[19] We will adopt this interpretation as detailed in Ref. 19 for the remainder of the discussion.

Ag deposition at the lowest coverage used [0.25 Ag(111) ML] was sufficient to cause removal of the surface-adatom feature from the Si $2p$ core line shape. This suggests that the $S2$ component has been modified by the presence of Ag to have a new binding energy much closer to those of the B and $S1$ components, and therefore cannot be resolved any more. The line shape changed negligibly at the higher Ag coverages studied (0.5 and 1 ML); therefore, these spectra are not shown here. Consequently, the addition of Ag does not appear to affect the $S1$ component. To analyze the data, the simplest assumption is that the $S2$ component is converted to have a binding energy the same as that of either the $S1$ component or the B component. Unfortunately, the Ag-covered surface spectra could not be fitted very well with these two-component fit models (see below). Thus it appears that the $S2$ component has a new, different binding energy from components B and $S1$. A fitting model involving three components was tried but failed to yield unique results. This is because the intensity and shift of $S2$ are small enough that they do not give rise to the separable, distinct spectral features required for a unique fit.

The top spectrum of Fig. 1 is therefore shown overlaid with one model prediction involving just two components. The components B and $S1$ have the same binding energies and line-shape parameters as the clean surface case. The relative intensity of component $S1$ is adjusted to correspond to the sum of the $S1$ and $S2$ emission from the clean surface. The solid line representing the composite model line shape is in reasonable correspondence with the experimental data. Another candidate model in which Ag adsorption causes the clean-surface $S2$ adatoms to become bulklike gave a slightly poorer correspondence with the data; it is not shown. Thus, it appears that the Ag adsorption causes the $S2$ component to move to a new binding energy closer to the $S1$ component than the B component, although it is not possible to determine precisely the new $S2$ energy position from the present set of data.

3. *Valence-band studies*

Photoemission spectra (unnormalized) from the valence bands of the clean Si(111)-(7×7) surface and the 0.25, 0.5, 1, and 2 ML Ag-covered Si(111) surfaces are shown in Fig. 2. The zero of the energy scale is the Fermi level.

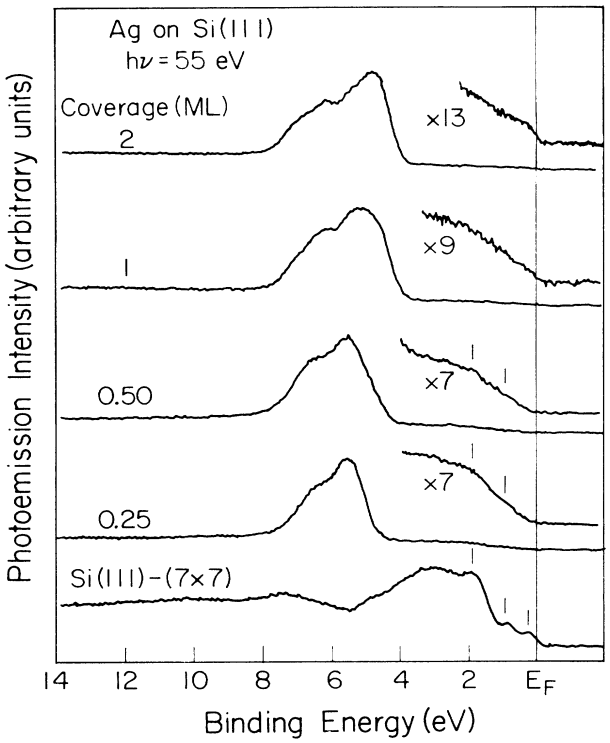

FIG. 2. Valence-band spectra for clean Si(111)-(7×7) and for surfaces with increasing Ag coverages at $h\nu = 55$ eV. These spectra are not normalized in intensity. To compare the intensities, the whole spectra, from bottom to top, should be amplified by factors of about 1, 6, 9, 14, and 17, respectively. Portions of the spectra have been amplified by the indicated arbitrary factors. Si(111)-(7×7) substrate surface-derived features are indicated by tic marks. The binding-energy scale is referred to the Fermi level E_F.

All of these spectra were taken at an incident photon energy of 55 eV. The scale factors needed to normalize the intensities of these spectra are given in the figure caption.

The clean Si(111)-(7×7) surface spectrum shows three surface states at approximately 0.3-, 0.9-, and 1.8-eV binding energy, indicated by tic marks in Fig. 2.[12–16] Other bulk-derived features are visible at higher binding energies. Recent advances in the use of STM have made it possible to obtain energy-resolved real-space images of filled and empty surface states of the Si(111)-(7×7) surface.[22] The STM data of Ref. 22 is consistent with the Takayanagi DAS model[23] and with reference to the same, shows the three surface states (in order of increasing binding energy) to originate from surface adatoms, the three regions between the six adatoms in each half of the unit cell where there are dangling bonds on the atoms in the layer beneath the adatoms and in the center of the corner holes, and adatom and corner-hole Si-Si backbonds.

Deposition of even a very small amount of Ag is sufficient to cause the valence-band spectra to be dominated by Ag emission features. The major spectral peaks 4—8 eV below E_F are derived from the Ag 4*d* bands. With 0.25 ML Ag coverage, the low- (0.3 eV) binding-energy surface state of Si(111)-(7×7) is suppressed and there is little emission at the Fermi level. The remnants of the features at 0.9- and 1.8-eV binding energies are still visible at this and slightly higher coverages as indicated by the tic marks in Fig. 2 (it is much easier to see these features with a greatly amplified scale). All substrate-derived features vanish at 1 ML coverage and a distinct Fermi edge is visible at 2 ML.

4. *Model*

Based on the above results, the simplest model for the initial growth of Ag on Si(111) is as follows. At 0.25 ML Ag coverage, the Ag atoms are bonded to the Si adatoms; thus the *S*2 core-level component is significantly shifted to a new energy position near that of the *S*1 component. The fairly large difference in binding energy between the *S*2 and *S*1 components for the clean Si(111)-(7×7) surface is mainly a result of the smaller coordination number for the adatoms. The adatom coordination number is increased by the attachment of Ag atoms; thus, the differences between *S*2 and *S*1 is greatly reduced for the Ag-coveraged surface. The surface state at 0.3-eV binding energy is completely eliminated at this coverage, but not the other two surface states. This result is consistent with the STM finding that the 0.3-eV state is mainly concentrated over the adatoms, and thus more susceptible to modification by the addition of Ag atoms. Note that the (7×7) HEED pattern is still observable at this coverage, indicating that the Si lattice below the adatom layer is not severely disrupted by the Ag adsorption. The higher HEED background can be easily explained by the lack of a single unique bonding configuration for the Ag atoms and/or the lack of long-range order for the Ag atom distribution.

With additional Ag coverage up to 1 ML, the core-level line shape shows negligible change, indicating that the *S*1 component is not sensitive to the presence of Ag. Presumably, the *S*1 atoms for the clean reconstructed surface are already in a fairly stable coordination configuration satisfying the requirement of chemical valence, which is not significantly changed by the addition of Ag. The two surface states at 0.9- and 1.8-eV binding energies become eliminated at higher Ag coverages because the additional Ag begins to populate the areas between the adatoms where these surface states have significant amplitude. As stated earlier, HEED is sensitive to essentially only the top atomic layer. Thus the visual disappearance of the (7×7) HEED pattern for coverages more than about 1 ML does not necessarily indicate that the reconstruction is completely eliminated. It may just be that the intensity of the $\frac{1}{7}$-order spots was too weak to be seen.

B. Ag on Ge(111)-*c*(2×8)

1. *HEED*

Electron diffraction patterns taken of the clean Ge(111) surface showed sharp $\frac{1}{8}$-order and $\frac{1}{2}$-order spots and a low background. The reconstruction was nominally *c*(2×8). The Ag deposition was performed at a substrate temperature of about 70°C. After deposition of 0.4

Ag(111) ML, the $\frac{1}{8}$-order features totally vanished and the $\frac{1}{2}$-order dots were barely visible. Ag(111) diffraction streaks appeared in parallel epitaxy with the substrate, accompanied by some weak extra diffraction streaks corresponding to domains rotated by 30° about the surface normal. Substrate- and overlayer-derived spots were of comparable intensity. The 0.8 ML Ag(111)-covered surface diffraction pattern contained sharper Ag(111) spots, very weak rotated (30°) domain lines, and weak Ge(111)-(1×1) substrate spots. At higher coverages (2 ML or more), the substrate was no longer visible. Ag(111) continued to grow in parallel epitaxy. No second-domain growth was observed. The HEED patterns were very sharp and indicated the presence of fairly flat and smooth Ag overlayers. At all of the coverages studied, no tilted Ag facets or three-dimensional structures were detected. Our observations are consistent with previous studies.[24] The growth behavior is very similar to that for Ag on Si(111)-(7×7) described above.

2. Core levels

Figure 3 shows high-resolution scans of the Ge 3*d* core level for Ge(111)-*c*(2×8), taken at incident photon energies of 40 eV (bottom), 70 eV (middle), and 90 eV (top). The 40-eV spectrum has the highest bulk sensitivity and the 90-eV spectrum the highest surface sensitivity. The data were analyzed by a procedure analogous to Ref. 19; in this case the 70- and 90-eV spectra were individually, simultaneously fit with the bulk-sensitive 40-eV spectrum. The results are displayed in Fig. 3 and tabulated in Table I. They are in excellent agreement with previous studies.[19,25] Again, a comparison of Table I in this paper with Table I of Ref. 19 shows that there is a high degree of reproducibility; the small differences provide an estimate of the uncertainty of our measurements. In Fig. 3, the component labeled *B* is derived from the bulk, and the components *S*1 and *S*2 are derived from the surface, following Ref. 19. The binding energies of all components are referred to the binding energy of the $3d_{5/2}$ core level of the *B* component in the bulk-sensitive 40-eV spectrum (29.42 eV, relative to the Fermi level).

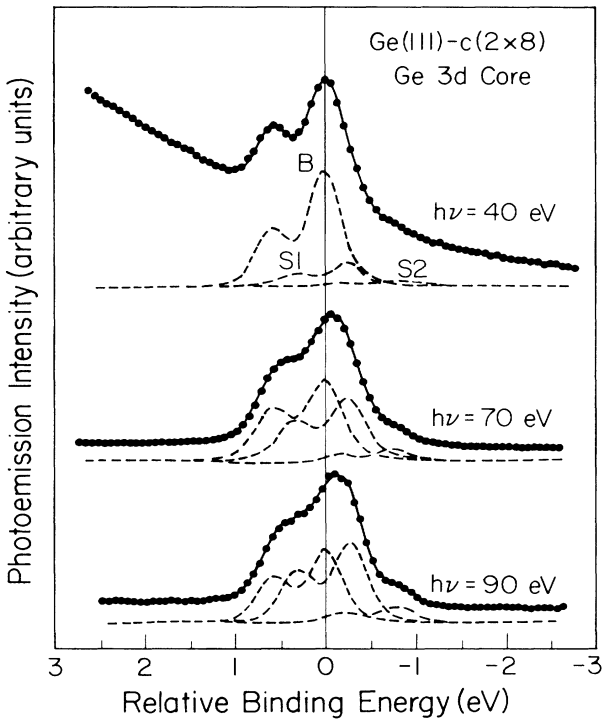

FIG. 3. Ge-3*d* core-level spectra for clean Ge(111)-*c*(2×8) taken at the indicated incident photon energies. The upper spectrum includes mainly emission from the bulk; the lower two emphasize surface features, with the 90-eV spectrum being the most surface sensitive. Circles are data points; the solid curves are fits to the data. The dashed curves represent the three spectral components; *B* is bulk in origin and *S*1 and *S*2 are surface derived. Binding energies are referred to component *B* of the Ge-$3d_{5/2}$ line.

The Ge(111)-*c*(2×8) surface was recently imaged with STM.[26] The surface structure, consisting of a combination of *c*(4×2) and (2×2) units, is not as well ordered as in the case of Si(111)-(7×7). The STM image consists of protrusions and depressions. If we assume the protrusions are adatoms, in analogy with the Si(111)-(7×7) case, Fig. 2 of Ref. 26 implies the adatom density corresponds to about 0.45 Ge(111) ML within the limited area imaged, the 10% departure from 0.5 ML being due to defects in the form of missing protrusions. One ML of Ge is defined here to be one-half of one double Ge(111) layer, or 7.2×10^{14} atoms/cm^2.

In analogy with the situation for Si(111)-(7×7), the low-binding-energy component *S*2 of the Ge 3*d* core line shape is likely to be derived from adatoms emission. Following the same analysis techniques described in Ref. 19 for the Si(111) case, we have estimated the equivalent coverage of the *S*2 component. For the 70-eV spectrum, the electron mean-free path is about 7.2 Å.[27] Because our angle-integrated photoemission geometry samples over many different exit angles, the effective escape depth is approximately 5.5 Å with an estimated uncertainty of ±0.5 Å.[27] This value of the escape depth leads to an equivalent coverage of 0.37±0.03 ML for the *S*2 adatom component. This value is smaller than the ideal value of 0.5 ML for a perfect *c*(2×8) structure because of the presence of defects on the surface. The STM result gives a value of about 0.45 ML as noted above. However, the STM picture was taken over a very small area; it is not clear whether this value is also typical over a macroscopic region. Thus, a fair comparison cannot be made based on the available results. Note that in the case of Si(111)-(7×7), the STM images typically show few defects; thus, there is a good correspondence between the measured *S*2 intensity and the ideal adatom coverage in this system. The intensity of peak *S*1 for the Ge 3*d* core line shape corresponds to emission from about 2.1 ML. The most likely interpretation of *S*1 is that it originates from the first full double layer beneath the adatoms. The relative energy position and intensity for *S*1 are different for Si(111) and Ge(111), an intriguing result already noted in Ref. 19.

Figure 4 shows high-resolution scans of the Ge 3*d* core

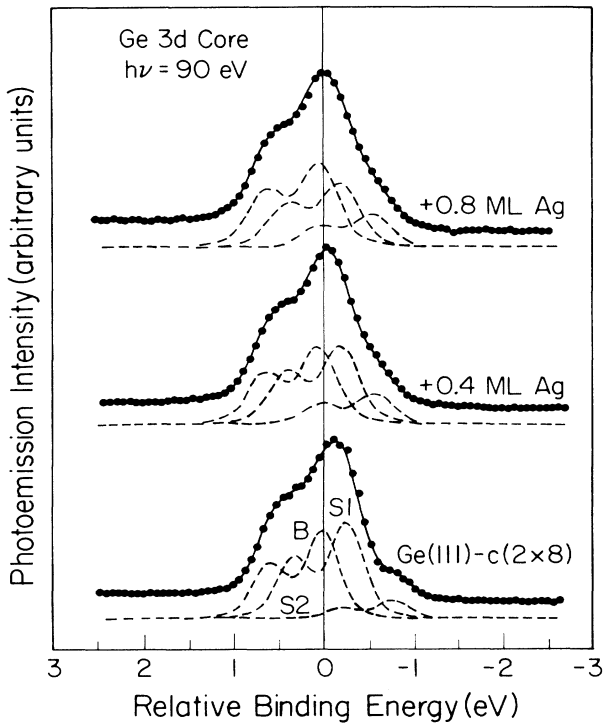

FIG. 4. Ge-3d core-level spectra for clean and Ag-covered Ge(111)-$c(2\times8)$ surfaces. The incident photon energy is 90 eV. Binding energies are referred to component B of the Ge-3$d_{5/2}$ line for the clean surface. The symbols are the same as Fig. 3.

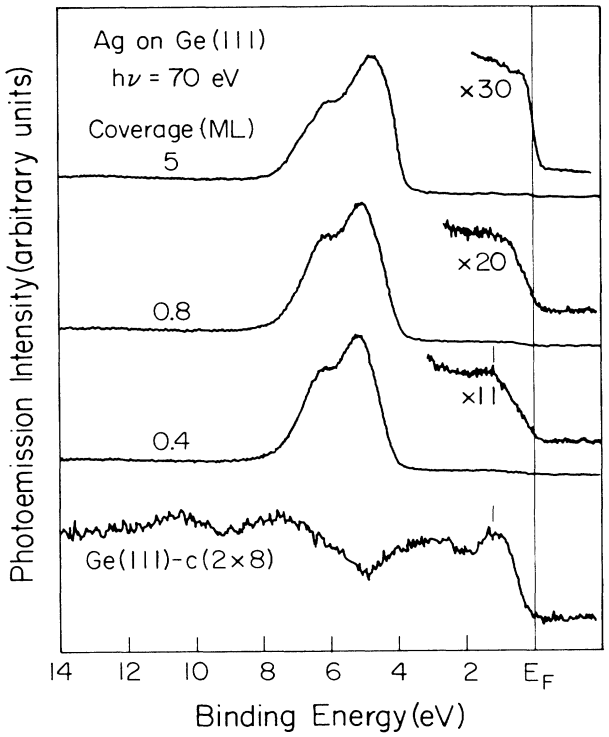

FIG. 5. Valence-band spectra for clean Ge(111)-$c(2\times8)$ and for surfaces with increasing Ag coverage at $h\nu=70$ eV. The spectra are not normalized in intensity. To compare intensities, the whole spectra, from bottom to top, should be amplified by factors of about 1, 30, 60, and 120, respectively. Portions of the spectra have been amplified by the indicated arbitrary factors. Ge(111)-$c(2\times8)$ substrate surface-derived features are indicated by tic marks. The binding-energy scale is referred to the Fermi level.

levels of three Ag-covered Ge(111) surfaces at an incident photon energy of 90 eV. From the bottom to top the Ag coverages are clean, 0.4 ML, and 0.8 ML Ag. As before, the data were analyzed by the procedure of Ref. 19; the surface-sensitive 90-eV spectra were simultaneously fit with bulk-sensitive 40-eV spectra (not shown) taken of the same system. Comparison of the bulk- and surface-sensitive cases again leads to the interpretation of component B as bulk derived and components $S1$ and $S2$ as from the surface. The binding energy reference is the same as Fig. 3. A small amount of band-bending (40 meV), causing the B component to shift, occurs upon Ag deposition; it is too small to be easily seen in the figure. The interpretation of the behaviors of the various components will be given below.

3. *Valence-band studies*

We display photoemission spectra from the valence bands of the clean Ge(111)-$c(2\times8)$ surface and the 0.4, 0.8, and 5 ML Ag-covered Ge(111) surfaces in Fig. 5. The zero of the energy scale is the Fermi level. The incident photon energy is 70 eV.

The clean Ge(111)-$c(2\times8)$ spectrum shows a feature at about 1.4-eV binding energy (denoted with a tic mark), which is derived from surface states.[15,16,28,29] It is also visible in the spectrum for 0.4 ML Ag coverage, although at this coverage the HEED pattern from the substrate is (1×1) instead of the $c(2\times8)$ for the clean surface. Thus, at least part of the surface-state emission is not sensitive to the long-range order, consistent with previous findings.[15,30] There is some emission at E_F in the submonolayer coverage spectra; the 5 ML spectrum has a well-defined Fermi edge. The major peaks 4—8 eV below E_F are derived from the Ag 4d bands.

4. *Model*

With 0.4 ML Ag on the surface, the $S2$ component of the core line shape (see Fig. 4) is shifted slightly towards the B component. As a result, the bump on the low-binding-energy side for clean Ge(111) becomes less distinct in the Ag-covered case. With further Ag coverage to a total of 0.8 ML, the position of $S2$ does not change. Its intensity relative to the B component, however, appears increased for increasing Ag coverages. Similar behaviors have been reported before for coverages in the range of 5—20 ML.[5] The $S1$ component, on the other hand, suffers a reduction in intensity relative to the B component for increasing Ag coverages.

As reported previously using a labeling technique,[5] high-resolution Ge 3d core-level studies of 5 ML or thicker Ag films on Ge(111) have shown that the Ge adatoms

tend to segregate on top of the growing Ag film. The data of Fig. 4 for lower coverages supports this view and provides additional information. Thus, at 0.4 ML Ag coverage (1 ML of Ag is approximately equivalent to 2 ML of Ge), the Ge adatoms are either floating on top of the Ag islands or are surrounded (but not covered) by the Ag atoms, resulting in a somewhat different binding energy closer to the B component. At 0.8 ML Ag coverage, most Ge adatoms are on top of the Ag layer. Since the photoemission signal from these Ge atoms are not attenuated by the Ag, the $S2$ intensity remains unchanged. The combined B and $S1$ intensity, on the other hand, is attenuated by the Ag overlayer. Therefore, the $S2$ intensity increases relative to that of the combined B and $S1$ components for increasing coverages. A detailed intensity analysis of the data supports the above qualitative description, but will not be presented here for simplicity.[5] The data in Fig. 4 shows that the reduction in the $S1$ intensity (relative to the B intensity) is proportional to the Ag coverage; by extrapolation, the $S1$ intensity is reduced to about $\frac{1}{2}$ of its original value for 1 ML Ag coverage. The $S1$ component for the clean surface corresponds to about 2 ML (1 full double layer) of Ge. Thus, one half of the $S1$ component, corresponding to 1 ML of Ge, is converted to have a bulklike binding energy for 1 ML of Ag coverage. At 1 ML Ag coverage, the Ge surface is essentially fully covered by Ag, since the growth of Ag(111) is fairly smooth. Disregarding the Ge adatoms which are now on top of the Ag ML, it is most likely that the top ML of the Ge substrate in contact with the Ag shows the original ($S1$) binding energy, while the second ML of Ge is converted to have a bulklike binding energy. This is a very reasonable assignment of the binding energies for different layers, but we cannot prove it definitively on the basis of the present data. The present data for low Ag coverages are entirely consistent with data reported previously for higher coverages.[5]

For comparison, we are not able to deduce similar information for the case of Ag on Si(111), namely, whether or not the Si adatoms on clean Si(111)-(7×7) segregate when Ag is deposited on the surface. This is because for Si(111) the $S2$ component is converted by Ag coverage to have a binding energy very close to that of the $S1$ component, and the two contributions cannot be reliably deconvolved. The behavior of the $S1$ component under Ag coverage is also quite different for the two systems.

C. Au on Ge(111)-$c(2\times8)$

1. HEED

Electron diffraction patterns taken of the clean Ge(111)-$c(2\times8)$ surface have been described above. Au was deposited on the surface at temperatures of about 70°C. Deposition of 0.1 ML Au increased background; the substrate $c(2\times8)$ pattern was still visible, but the $\frac{1}{8}$-order features were somewhat obscured. One ML of Au is defined here as an atomic layer in Au(111), or 1.37×10^{15} atoms/cm^2. At 0.5 ML coverage, the pattern contained indistinct Ge(111)-(1×1) dots with wide streaks around them of modulated intensity, and high background. The $\frac{1}{2}$- and $\frac{1}{8}$-order spots were no longer visible. The 2 ML-covered surface showed weak Ge(111)-(1×1) dots, some diffuse lines, and high background. Additional, faint, and very broad streaks in the diffraction pattern were always present regardless of sample orientation, a sign of randomly oriented clusters of islands. Thus, the Au overlayer with a thickness larger than a ML shows substantial disorder, in sharp contrast to the behaviors for the other two systems discussed above. Similar results have been obtained in previous studies.[3,31]

2. Core levels

Figure 6 shows high-resolution scans of the Ge 3d core levels for clean Ge(111) and two Au-covered Ge(111) surfaces taken at an incident photon energy of 90 eV. From bottom to top the Au coverages are clean Ge(111)-$c(2\times8)$, 0.1 ML, and 0.5 ML Au. The deconvolution of the clean spectrum has been described above and the results of the fit are shown in Fig. 6 by the solid curve (fit to the overall line shape) and the dashed curves (individual contributions from the bulk and the two surface components).

The 0.1 Au ML-covered surface core-level line shape in Fig. 6 is very similar to that of the clean surface, except that the low-binding-energy shoulder ($S2$ contribution) is smaller and appears to have shifted somewhat toward the $S1$ or B component. The outcome of the fitting procedure for this line shape assuming three components only

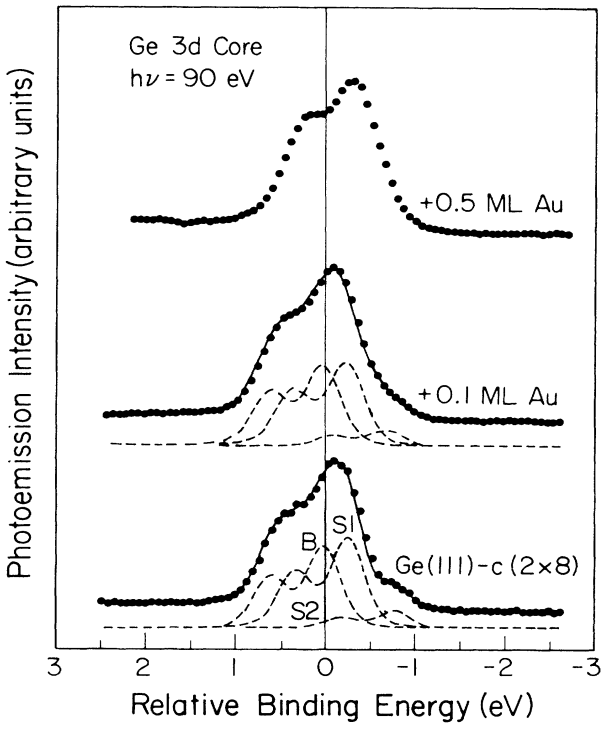

FIG. 6. Ge-3d core-level spectra for clean and Au-covered Ge(111)-$c(2\times8)$ surfaces. The incident photon energy is 90 eV. Binding energies are referred to component B of the Ge-3$d_{5/2}$ line for the clean surface. The symbols are the same as Fig. 3.

is displayed in the figure. The quality of the fit is quite good. However, we are uncertain whether or not the system can be accurately described by only three components. Assuming the fit result reflects the actual physical situation, the simplest interpretation of the data is that the $S2$ adatoms are affected by the Au adatoms such that the binding energy is shifted to a value closer to that of the B or $S1$ component, in analogy to the situation for Ag on Si(111) discussed above. One ML of Au has about twice the number of atoms than one ML of Ge, and each Au atom could affect two Ge adatoms if the Au atom is bonded to both. Thus, it is entirely possible that 0.1 ML of Au could cause all the $S2$ Ge adatoms to shift.

The low-binding-energy shoulder is no longer visible in the 0.5 ML line shape in Fig. 6. The spectrum roughly has the appearance of two unresolved peaks. Notice the intensity ratio of the two peaks is now different than the other two spectra and the corresponding case for the Ag-on-Ge system. The Ge $3d$ core line shape for the 2 ML Au-covered surface (not shown) is very similar. Note that there is an overall shift of the center of gravity of the line shape for 0.5 ML coverage, indicating a significant change in band bending induced by Au adsorption. We have attempted to fit the line shape of the top spectrum in Fig. 6 using many different models involving different numbers of components, but none of these fits is satisfactory unless we allow the intensity branching ratio between the spin-orbit-split pairs to be significantly different from that for the clean case. If this assumption is made, then the spectrum can be fit well with just two components; a three-component fit does not give unique results. HEED results showed that this system is substantially disordered, a situation different from that for Ag on Ge; this suggests that there may be a reaction or intermixing between Au and Ge. Perhaps the interaction between Au and Ge is so strong that the electronic properties of Ge are significantly modified, leading to a different branching ratio. This is just one conjecture. We do not have a definitive explanation for this problem, and we are unaware of any reliable, quantitative theory relating the branching ratio to the local chemistry.

3. *Valence-band studies*

Valence-band photoemission spectra from the clean Ge(111)-$c(2\times8)$ surface and (from bottom to top) the 0.1, 0.5, and 2 ML Au-covered surfaces are shown in Fig. 7. The zero of the energy scale is the Fermi level. The incident photon energy is 70 eV. The 1.4-eV Ge(111)-$c(2\times8)$ surface-state feature is visible in the bottom spectrum. It is still present in the 0.1 ML spectrum. The feature disappears at higher coverages. The DOS is very small at E_F; at no point is a clearly defined Fermi edge visible. This result is consistent with the fact that no pure-Au-derived HEED spots were observed for this system. Thus, even at 2 ML Au coverage, the Au does not form a pure Au layer or clusters that give rise to a sharp Fermi edge (for comparison, see Fig. 2). This again implies a reaction or intermixing between the Au and Ge. The two major peaks between 4 and 8 eV are derived from the Au $5d$ states.

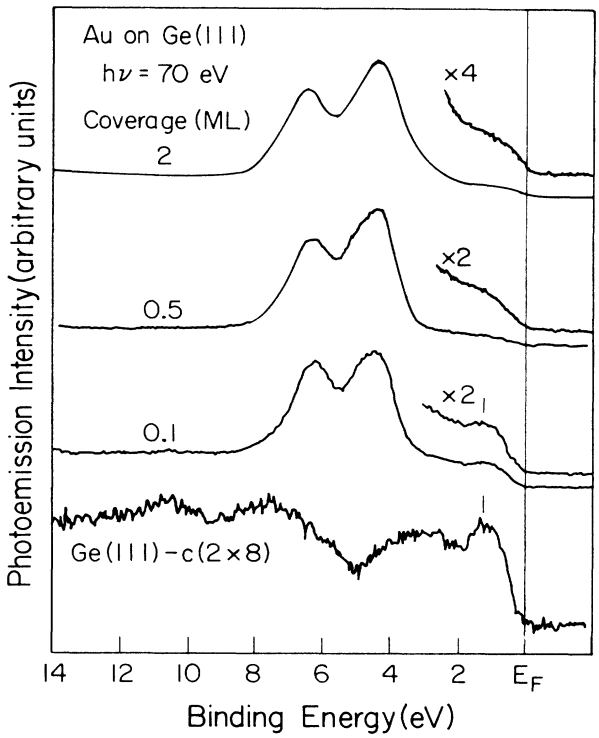

FIG. 7. Valence-band spectra for clean Ge(111)-$c(2\times8)$ and for surfaces with increasing Au coverages at $h\nu=70$ eV. The spectra are not normalized in intensity. To compare intensities, the whole spectra, from bottom to top, should be amplified by factors of about 1, 4, 20, and 40, respectively. Portions of the spectra have been amplified by the indicated arbitrary factors. Ge(111)-$c(2\times8)$ substrate-derived features are indicated by tic marks. The binding-energy scale is referred to the Fermi level.

4. *Model*

From the evidence provided above, the initial adsorption of Au on Ge(111) (0.1 ML coverage) is likely to involve bonding to the Ge adatoms leading to a core-level binding-energy shift for the Ge adatoms. At higher coverages, there is evidence for a strong interaction between the Au and Ge. The growth is disordered, and the experimental results suggest a reaction or intermixing between the overlayer and substrate.

IV. SUMMARY AND CONCLUSIONS

We have performed electron diffraction and high-resolution core-level and valence-band photoemission investigations of the initial growth of Ag on Si(111)-(7×7), Ag on Ge(111)-$c(2\times8)$, and Au on Ge(111)-$c(2\times8)$. Our results show correlations between structural and electronic properties. They support certain substrate surface structural models and have implications for possible Au and Ag adsorption models upon these surfaces.

Specifically, the data for the Ag on Si(111)-(7×7) system suggests the low-binding-energy (0.3-eV) surface state is closely related to the $\frac{12}{49}$ ML of surface adatoms. Emission from this state is correlated with the presence of the

low-binding-energy shoulder in the Si $2p$ core-level line shape. The result is in accordance with the Takayanagi DAS model and recent STM studies. The initial bonding of Ag is to the Si adatoms, resulting in a selective modification of the adatom-derived core-level component and the 0.3-eV surface state. The 0.9- and 1.8-eV surface states are eliminated only for higher coverages when the space between the adatoms becomes filled. The Ag-on-Ge(111) system behaves differently in certain aspects. The clean Ge surface has a substantial number of defects in the form of missing adatoms, and two atomic layers below the adatoms have shifted core-level binding energies. The Ag adsorption modifies the Ge adatom binding energy, and for sufficient Ag coverages, the Ge adatoms segregate to the top of the growing Ag film. Simultaneously, the atomic layer just below the substrate surface layer is modified to show a bulklike core-level binding energy. For both Ag-on-Si(111) and Ag-on-Ge(111) systems, Ag(111) islands are formed for submonolayer coverages. The Ag(111) overlayer is fairly smooth at higher coverages, although the growth mode is not exactly laminar. The Au-on-Ge system, on the other hand, exhibits a strong interaction between the overlayer and the substrate such that the system shows a disordered growth behavior. This stronger interaction is inferred from the lack of a well-developed Fermi edge in the valence DOS spectrum, HEED patterns indicating a disordered growth, and the core-level line shape indicating possibly a significantly modified spin-orbit branching ratio.

ACKNOWLEDGMENTS

This material is based upon work supported by the U.S. Department of Energy (Division of Materials Sciences), under Contract No. DE-AC02-76ER01198. Some of the equipment used for this research was obtained with grants from the National Science Foundation (Grant No. DMR-83-52083, DMR-83-11281, and DMR-86-14234), the IBM Thomas J. Watson Research Center (Yorktown Heights, NY), the Hewlett Packard Laboratories, and the Central Research Department of the E. I. du Pont de Nemours and Company. The Synchrotron Radiation Center of the University of Wisconsin—Madison is supported by the National Science Foundation under Contract No. DMR-80-20164. We acknowledge the use of central facilities of the Material Research Laboratory of the University of Illinois, which is supported by the U.S. Department of Energy (Division of Materials Sciences), under Contract No. DE-AC02-76ER01198, and the National Science Foundation under Contract No. DMR-80-20250.

[1]L. J. Brillson, Surf. Sci. Rep. **2**, 123 (1982) and references therein.

[2]*Thin Films: Interdiffusion and Reactions*, edited by J. M. Poate, and K. N. Tu, and J. W. Mayer (Wiley, New York, 1978); G. Ottaviani, K. N. Tu, and J. W. Mayer, Phys. Rev. B **24**, 3354 (1981).

[3]G. LeLay, Surf. Sci. **132**, 169 (1983), and references therein.

[4]M. Hanbucken, M. Futamoto, and J. A. Venables, Surf. Sci. **147**, 433 (1984).

[5]A. L. Wachs, T. Miller, and T.-C. Chiang, Phys. Rev. B **33**, 8870 (1986).

[6]A. L. Wachs, A. P. Shapiro, T. C. Hsieh, and T.-C. Chiang, Phys. Rev. B **33**, 1460 (1986).

[7]A. L. Wachs, T. Miller, and T.-C. Chiang, Phys. Rev. B **29**, 2286 (1984).

[8]T. Miller, E. Rosenwinkel, and T.-C. Chiang, Phys. Rev. B **30**, 570 (1984).

[9]See, for example, P. H. Citrin, and G. K. Wertheim, Phys. Rev. B **27**, 3176 (1983).

[10]T.-C. Chiang, G. Kaindl, and T. Mandel, Phys. Rev. B **33**, 695 (1986).

[11]T. C. Hsieh, T. Miller, and T.-C. Chiang, Phys. Rev. B **33**, 2865 (1986); T. C. Hsieh, A. P. Shapiro, and T.-C. Chiang, *ibid.* **31**, 2541 (1985).

[12]F. J. Himpsel *et al.*, Phys. Rev. B **24**, 1120 (1981); F. J. Himpsel, Physica **117&118B**, 767 (1983).

[13]H. Neddermeyer, U. Misse, and P. Rupieper, Surf. Sci. **117**, 405 (1982); G. V. Hansson and S. A. Floodstrom, J. Vac. Sci. Technol. **16**, 1287 (1979).

[14]J. E. Demuth, B. N. J. Persson, and A. J. Schell-Sorokin, Phys. Rev. Lett. **51**, 2214 (1983).

[15]A. L. Wachs, T. Miller, T.-C. Hsieh, A. P. Shapiro, and T.-C. Chiang, Phys. Rev. B **32**, 2326 (1985).

[16]T. Miller, T.-C. Hsieh, P. John, A. P. Shapiro, A. L. Wachs, and T.-C. Chiang, Phys. Rev. B **33**, 4421 (1986).

[17]G. LeLay, M. Manneville, and R. Kern, Surf. Sci. **72**, 405 (1978); M. Hanbucken, H. Neddermeyer, and P. Rupieper, Thin Solid Films **90**, 37 (1982); G. Dufour, J.-M. Mariot, A. Masson, and H. Roulet, J. Phys. C **14**, 2539 (1981); F. Houzay, G. M. Guichar, A. Cros, F. Salvan, R. Pinchaux, and J. Derrien, Surf. Sci. **124**, L1 (1983); Y. Gotoh and S. Ino, Jpn. J. Appl. Phys. **17**, 2097 (1978).

[18]F. J. Himpsel, P. Heimann, T.-C. Chiang, and D. E. Eastman, Phys. Rev. Lett. **45**, 1112 (1980).

[19]T. Miller, T. C. Hsieh, and T.-C. Chiang, Phys. Rev. B **33**, 6983 (1986).

[20]G. Binnig, H. Rohrer, Ch. Gerber, and E. Weibel, Phys. Rev. Lett. **50**, 120 (1983).

[21]R. S. Becker, J. A. Golovchenko, E. G. McRae, and B. S. Schwarzentruber, Phys. Rev. Lett. **55**, 2028 (1985); R. S. Becker, J. A. Golovchenko, D. R. Hamann, and B. S. Schwarzentruber, *ibid.* **55**, 2032 (1985).

[22]R. J. Hamers, R. M. Tromp, and J. E. Demuth, Phys. Rev. Lett. **56**, 1972 (1986).

[23]K. Takayanagi, Y. Tanishiro, M. Takahashi, and S. Takahashi, J. Vac. Sci. Technol. A **3**, 1502 (1985).

[24]M. Bertucci, G. LeLay, M. Manneville, and R. Kern, Surf. Sci. **85**, 471 (1979).

[25]S. B. DiCenzo, P. A. Bennett, D. Tribula, P. Thiry, G. K. Wertheim, and J. E. Rowe, Phys. Rev. B **31**, 2330 (1985).

[26]R. S. Becker, J. A. Golovchenko, and B. S. Schwarzentruber, Phys. Rev. Lett. **54**, 2678 (1985).

[27]T. Miller, A. P. Shapiro, and T.-C. Chiang, Phys. Rev. B **31**, 7915 (1985).

[28]J. M. Nicholls, G. V. Hansson, R. I. G. Uhrberg, and S. A. Floodstrom, Phys. Rev. B **33**, 5555 (1986).
[29]R. D. Bringans and H. Hochst, Phys. Rev. B **25**, 1081 (1982).
[30]F. J. Himpsel, D. E. Eastman, P. Heimann, B. Reihl, C. W. White, and D. M. Zehner, Phys. Rev. B **24**, 1120 (1981).
[31]G. LeLay, M. Manneville, and J. J. Metois, Surf. Sci. **123**, 117 (1982).